



**HAL**  
open science

## Practical adhesion measurements of protective coatings on bronze by three-point bending test

Maëlen Aufray, Claudie Josse, Andrea Balbo, Cecilia Monticelli, Erika Švara Fabjan, Luka Škrlep, Tadeja Kosec, Nina Gartner, Carla Martini, Giulia Masi,  
et al.

### ► To cite this version:

Maëlen Aufray, Claudie Josse, Andrea Balbo, Cecilia Monticelli, Erika Švara Fabjan, et al.. Practical adhesion measurements of protective coatings on bronze by three-point bending test. *Journal of Coatings Technology and Research*, 2019, 16 (5), pp.1465-1477. 10.1007/s11998-019-00230-5 . hal-02535686

**HAL Id: hal-02535686**

**<https://hal.science/hal-02535686>**

Submitted on 7 Apr 2020

**HAL** is a multi-disciplinary open access archive for the deposit and dissemination of scientific research documents, whether they are published or not. The documents may come from teaching and research institutions in France or abroad, or from public or private research centers.

L'archive ouverte pluridisciplinaire **HAL**, est destinée au dépôt et à la diffusion de documents scientifiques de niveau recherche, publiés ou non, émanant des établissements d'enseignement et de recherche français ou étrangers, des laboratoires publics ou privés.



## Open Archive Toulouse Archive Ouverte (OATAO)

OATAO is an open access repository that collects the work of Toulouse researchers and makes it freely available over the web where possible

This is an author's version published in: <http://oatao.univ-toulouse.fr/25838>

**Official URL:** <https://doi.org/10.1007/s11998-019-00230-5>

**To cite this version:**

Aufray, Maëlen<sup>ORCID</sup> and Josse, Claudie<sup>ORCID</sup> and Balbo, Andrea ,... [et al.] *Practical adhesion measurements of protective coatings on bronze by three-point bending test.* (2019) *Journal of Coatings Technology and Research*, 16 (5). 1465-1477. ISSN 1547-0091

Any correspondence concerning this service should be sent to the repository administrator: [tech-oatao@listes-diff.inp-toulouse.fr](mailto:tech-oatao@listes-diff.inp-toulouse.fr)

# Practical adhesion measurements of protective coatings on bronze by three-point bending test

Maëlen Aufray , Claudie Josse, Andrea Balbo, Cecilia Monticelli, Erika Švara Fabjan, Luka Škrlep, Tadeja Kosec, Nina Gartner, Carla Martini, Giulia Masi, Cristina Chiavari, Elena Bernardi, Maria Chiara Bignozzi, Luc Robbiola, Marija Babnik, Teja Koršič, Marko Kete

**Abstract** When attempting to sufficiently protect outdoor bronze monuments from corrosion, searches for an effective solution are usually based on coating applications which have a high anticorrosive efficiency. In order to correctly assess the level of protection provided by such coatings, adherence (practical adhesion) measurements need to be performed for the proper evaluation of the deterioration of coating systems with aging. Although a coupled study of adherence with aging would be of great interest, very few such studies are available. In this work, a methodological approach is proposed for the evaluation of coatings applied to metallic cultural heritage monuments of, based on the use of a three-point bending

test. Adherence characterization of different protective coatings has been performed both on bare and on traditionally black-patinated bronze coupons (Cu–Sn alloy with 5.9 wt% Sn), which were used as basic model substrates. The investigated coatings were Incralac<sup>®</sup>, silane, sol–gel oxysilane, and a silane-modified polymethacrylate (an adhesion promoter for fluoropolymer). The results of measurements which were obtained before and after accelerated aging in concentrated acid rain made it possible to more easily differentiate between the various adherence levels of different coating systems. Coupled with adherence measurements, the results of systematic optical and SEM observation of the different failure morphologies

M. Aufray (✉), M. Babnik, T. Koršič, M. Kete  
CIRIMAT, Université de Toulouse, CNRS,  
INP- ENSIACET 4 allée Emile Monso - BP44362,  
31030 Toulouse Cedex 4, France  
e-mail: maelenn.aufray@ensiacet.fr

M. Babnik  
e-mail: Marija@tempus-babnik.si

T. Koršič  
e-mail: teja@geida.si

M. Kete  
e-mail: marko@geida.si

C. Josse  
Centre de Microcaractérisation Raimond Castaing (CNRS  
UMS 3623), Université Fédérale de Toulouse,  
31000 Toulouse, France  
e-mail: claudie.josse@ensiacet.fr

A. Balbo, C. Monticelli  
Centro di Studi sulla Corrosione e Metallurgia “A. Daccò”,  
Università di Ferrara, 44121 Ferrara, Italy  
e-mail: andrea.balbo@unife.it

C. Monticelli  
e-mail: mtc@unife.it

E. Švara Fabjan, L. Škrlep, T. Kosec, N. Gartner  
Slovenian National Building and Civil Engineering Institute,  
Dimičeva 12, 1000 Ljubljana, Slovenia  
e-mail: erika.svara-fabjan@zag.si

L. Škrlep  
e-mail: luka.skrlep@zag.si

T. Kosec  
e-mail: tadeja.kosec@zag.si

C. Martini  
Dipartimento di Ingegneria Industriale, Università di  
Bologna, viale del Risorgimento 4, 40136 Bologna, Italy  
e-mail: carla.martini@unibo.it

G. Masi, M. C. Bignozzi  
Dipartimento di Ingegneria Civile, Chimica, Ambientale e  
dei Materiali, Università di Bologna, Via Terracini, 28,  
40131 Bologna, Italy  
e-mail: giulia.masi5@unibo.it

M. C. Bignozzi  
e-mail: maria.bignozzi@unibo.it

are also presented. In the case of the coated bare alloy, adhesive failures were mainly observed. The silane (PropS-SH) coating showed the best adherence. In the case of the patinated bronze test specimens, only cohesive failures occurred. Adherence is directly related to the cohesion of the black patina rather than that of the applied coating. It was observed that aging reduces the level of the adherence.

**Keywords** Adherence, Practical adhesion, Patina, Aging, FIB-SEM, Outdoor bronze, Conservation, Cultural heritage

## Introduction

Protection of cultural heritage is an important topic, in which specific scientific approaches have to be applied. In the challenging field of the conservation and maintenance of structures and other objects, advanced protection strategies are needed in order to reduce maintenance costs and to design efficient conservation solutions. Metallic artifacts, such as bronze statues or monuments, particularly those exposed to outdoor conditions in urban environments, are prone to marked degradation processes.<sup>1</sup> In such cases, their protection by means of overlying coatings is still one of the best available solutions.<sup>2,5</sup> Most investigations for the development of better corrosion protection are focused on protective coatings with a high anticorrosion efficiency.<sup>4,5</sup> However, surface protection depends on several properties, and not only on the barrier effect or inhibition efficiency of individual applied coatings. The adherence properties of coating/patina/metal systems need to be considered if an adequate conservation strategy is to be developed. The assessment of adherence is thus a key point for the characterization of the protective efficiency of coating systems. Coupled studies of adherence with accelerated aging are also of great interest for the assessment of the long-term

behavior of coatings.<sup>6–12</sup> In cultural heritage studies aimed at the conservation of ancient metallic materials<sup>1</sup> the stability and good adhesion of coatings after aging in condensed moisture conditions is difficult to achieve. Such a combined approach could be very important, although so far it has not really been investigated thoroughly. Adherence (or practical adhesion/adhesion strength) is usually assessed by means of tests which measure the resistance of the coating–substrate interface to mechanical damage. The difference between practical adhesion and basic adhesion (i.e., the physical and/or chemical bonding across the coating/substrate interface, which is often difficult to measure) is well known and has been widely discussed in previous works.<sup>13–15</sup> In fact, most adhesion tests do not measure this basic adhesion but produce a practical adhesion measurement, also called adherence, combining together the basic adhesion with other factors which can be specific for a given material, pair of materials, or a given test method. In this work, the expressions “practical adhesion” and “adherence” will be deemed to have the same meaning. Conventional methods such as progressive load scratch tests<sup>13,16</sup> or indentation methods,<sup>17–21</sup> which are widely used in the case of thin hard coatings on metallic substrates, are not suitable for application to thin polymeric films such as those investigated in this work. Pull-off tests have been applied to a wide range of coating/substrate systems.<sup>22</sup> However, when assessing the practical adhesion of protective layers for metals belonging to the cultural heritage, where the behavior of the coating during exposure to a corrosive environment has to be taken into consideration, none of these tests yields satisfactory results. In particular, the results of pull-off tests depend on the selected area, which is not easy to control. Moreover, failure may not occur at the metal–polymer interface, so that the test cannot be considered to be a “true” adherence test.<sup>23–25</sup> Apart from all of this, it is not possible to separate the location of the failure initiation from the propagation zone. For this reason, a high-accuracy adherence test was applied and is discussed in this work. Specifically, the practical adhesion of protective coatings applied to either bare or black-patinated Cu–6Sn bronze substrates was determined by means of a three-point bending test, using an epoxy stiffener. Developed by Roche et al.,<sup>23,25</sup> the three-point bending test provides a quantifiable parameter for characterising adherence and makes it possible for the failure initiation site to be more easily observed. When carried out before and after accelerated aging, this test enables better differentiation between the various adherence levels.<sup>23–25</sup>

This study formed part of a larger scientific program, M-Era.Net European project BIMPACT (Bronze-IMproved nonhazardous PATina CoaTings), which was aimed at the development of innovative eco-friendly and nonhazardous protective coatings for the protection of outdoor bronze statues or other monuments.

C. Chiavari  
Dipartimento di Beni Culturali, Università di Bologna, Via degli Ariani, 1, 48121 Ravenna, Italy  
e-mail: cristina.chiavari@unibo.it

E. Bernardi  
Dipartimento di Chimica Industriale “Toso Montanari”, Università di Bologna, Viale del Risorgimento 4, 40136 Bologna, Italy  
e-mail: elena.bernardi@unibo.it

L. Robbiola (✉)  
TRACES Lab, CNRS (UMR5608), Université Toulouse, 31058 Toulouse, France  
e-mail: robbiola@univ-tlse2.fr

M. Babnik, T. Koršič, M. Kete  
GEIDA, Zapogje 37, 1217 Vodice, Slovenia

A number of different protective coatings suitable for both bare and black-patinated bronze were investigated:

1. Alkyl-silane coatings: 3-mercaptopropyltrimethoxysilane (PropS-SH)-based coatings were selected since they provide excellent protection against the corrosion of copper and bronze.<sup>26–28</sup>
2. A sol-gel coating (SG): its formulation consists of a complex mixture including several ethoxysilanes, which were chosen due to their low curing temperatures, good protection against corrosion, and mechanical stability.<sup>29</sup>
3. A silane-modified adhesion promoter (MS) for fluoroacrylate-based coatings: this was a poly(fluoroacrylate) which exhibited good water-repellent properties and outdoor durability, but its adherence to different materials can be poor.<sup>30</sup> For this reason, a copolymer consisting of methyl methacrylate and methacryloxypropyltrimethoxysilane, abbreviated as MS, was tested as an adhesion promoter due to its expected good adhesion with the fluoroacrylate polymer, its good adhesion to bronze surfaces, and its excellent cohesion because of the siloxane crosslinks which it contains.<sup>5,31</sup>

Additionally, a commercial coating, Incralac<sup>®</sup>, which has been frequently used for the conservation of outdoor monuments for a number of decades,<sup>32,33</sup> was used as reference protective coating. Incralac<sup>®</sup> is a methyl methacrylate/ethyl methylacrylate copolymer, with benzotriazole as a corrosion inhibitor, which is dissolved in aromatic solvents.

In this work, the proposed methodology for adherence investigation was applied on a wrought tin bronze plate (Cu-6Sn), which was used as the model substrate. Characterization of the coating's practical adhesion was performed on bare bronze as well as on black-patinated bronze coupons (the artificial patina was produced by the traditional K<sub>2</sub>S method,<sup>33,34</sup> both before and after accelerated aging).

Accelerated aging of the coated substrates was carried out by immersion in a concentrated synthetic acid rain solution for 28 days, based on the composition of natural acid rain.<sup>35,36</sup> After the three-point bending tests had been performed, surface characterization was carried out by optical and electronic microscopy. In situ cross sections produced by Focused ion beam (FIB) milling was observed by FEG-SEM, in order to identify the failure modes which occurred in the three-point bending tests.

## Experimental

### Materials

#### Bronze (Cu-6Sn)

A Cu-6Sn wrought commercial bronze (EN1652 CW452K, which is equivalent to UNS C51900) was

used, corresponding to 0.5-mm-thick rolled plates. This tin bronze was a homogenized alpha Cu(Sn) solid solution with an Sn content of  $5.9 \pm 0.1$  wt% (3.25 at.%), determined from its lattice parameter (0.3649 nm) measured by X-ray diffraction by applying Vegard's law.<sup>37</sup> Other elements were present in very small amounts: < 0.2 wt% (P, Ni and Zn), < 0.1 wt% Fe and < 0.02 wt% Pb, based on the supplier's information.

### Black patination

One set of bronze plates was black-patinated (the "P" samples), whereas another set was kept untreated (bare bronze: the "B" samples) to be used as a reference. The black patina was applied on bare bronze by means of a torch technique in a manner which was similar to that traditionally used by nineteenth-century French *patineurs* for large statues, and which is still in use today.<sup>33,34</sup> The bronze was preheated up to around 100°C on a hotplate so that its heating condition was homogenized. An aqueous solution of potassium sulfide (K<sub>2</sub>S 3 wt%) was then directly applied with a brush until a brownish black color developed. After cooling, the surface was rinsed under tap water.

At the microscale level, the black patina consists of very small grains of micrometric size, which form a rough uniform layer, as shown in Figs. 1a and 1b, due to the formation of copper sulfide and cuprous oxide.<sup>34,38</sup> Both Cu<sub>2</sub>S (chalcocite) (JCPDS PDF 00-073-6087 and 00-026-1116) and Cu<sub>2</sub>O (JCPDS PDF 01-071-3645) were identified by means of grazing angle X-ray diffraction.

As shown Figs. 1c and 1d, the artificial black patina is 1 to 3 μm thick and consists of successive layers containing O, S and Cu, which are linked to the hot patination process. The patina is characterized by its multilayer structure,<sup>34</sup> which includes internal cuprous oxide and external cuprous sulfide, due to the selective dissolution of Cu, oxidized tin remaining in the internal layer as similarly observed in the case of patinas on corroded bronze.<sup>39</sup>

### Coatings

The protective coatings tested within the BIMPACT project (Table 1) were applied on bare (B) and patinated (P) bronze coupons. Their preparation details are as follows:

1. The alkyl-silane coatings: 3-mercaptopropyltrimethoxysilane (PropS-SH)-based coatings, plain and inhibitor-containing, were obtained by dissolving PropS-SH (purity 95%, Aldrich) in a hydroalcoholic solution (90/5/5 v/v ethanol/water/PropS-SH). This was acidified to pH 4 by the addition of some drops of diluted sulfuric acid solution and waiting 24 h at room temperature for

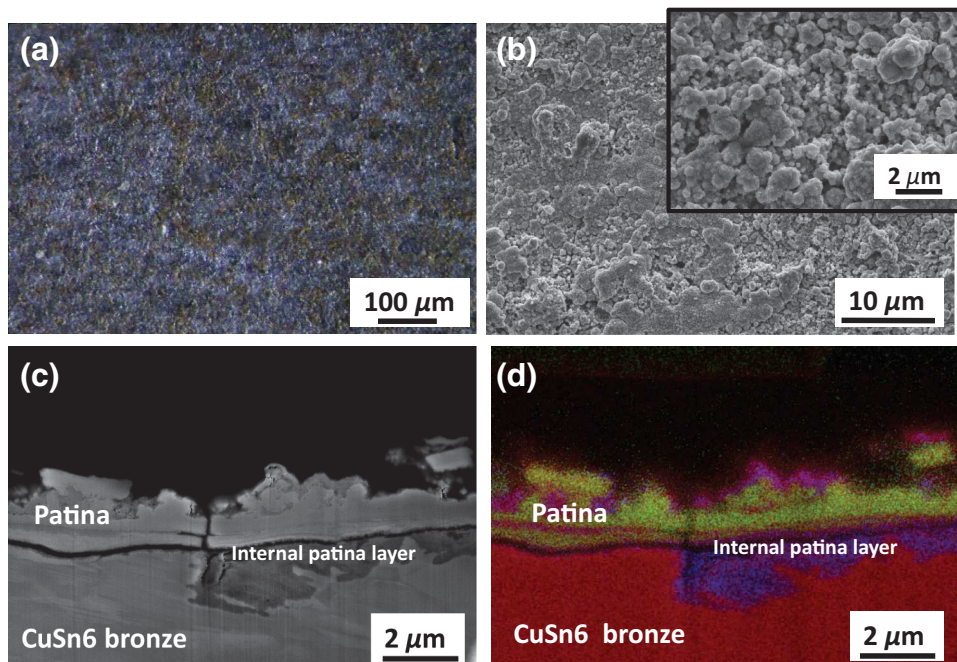


**Fig. 1:** Typical surface of black  $K_2S$  patina on Cu-6Sn bronze: (a) optical, (b) SEM images, with details of the morphology of the patina, (c) a cross section from FIB-SEM, and (d) the corresponding RGB image of Cu (red), S (green), and O (blue) X-ray maps: the patina layer is formed by Cu-S and Cu-O species—within the bronze (in red), a Cu depletion and a relative tin enrichment (in violet) induced by the patination process can also be seen (Color figure online)

silane hydrolysis. Then, in the case of the inhibitor-containing coatings, 5-mercapto-1-phenyl-tetrazole (MPT) was added to the hydrolyzed silane solution in the form of a  $\beta$ -cyclodextrin (CD) complex, which was prepared by mixing MPT and CD in equimolecular proportion in an aqueous solution. The final MPT concentration in the hydrolyzed solution was 0.5 mM. In all cases, the silane solutions were sprayed to a specific coating weight of about  $6 \text{ g m}^{-2}$ .

2. The sol-gel coating (SG): this was a complex mixture which included several ethoxysilane, making it easy to apply to bronze. The sol-gel coating was prepared by adding 0.2 mL of 3-glycidoxypropyltrimethoxysilane (GPTMS) and a small amount of zirconium(IV) butoxide ( $40 \mu\text{L}$ ) to a 1-propanol dispersion of highly hydrophobic silica particles (HMFS), 1 g in 40 mL of 1-propanol. The mixture was stirred for 4–6 h. After this,  $56 \mu\text{L}$  of methyltrimethoxysilane (MTMS),  $50 \mu\text{L}$  of water, and  $4 \mu\text{L}$  of HCl (37%) were gradually added. The sol-gel solution was left to hydrolyze for 24 h. After application (by brush or spray), the coating was cured at  $150^\circ\text{C}$  for 1 h.
3. The methyl methacrylate (MS) was obtained from Akripol, and 3-methacryloxypropyltrimethoxysilane was provided by ABCR GmbH. The lauroyl peroxide and diethylsuccinate were obtained from Sigma Aldrich. The synthesis of the silane-modified adhesion promoter was by means of a batch reaction, combining the random copolymers of

methyl methacrylate and methacryloxypropyltrimethoxysilane at a ratio of 9:1. Acetone was used as the solvent, and 2% lauroyl peroxide was used as an initiator. The combined monomer concentration was 10% (based on the condensed form of silane). The reaction temperature was  $55^\circ\text{C}$ , and the reaction time was 72 h. After the reaction, diethylsuccinate was added to the reaction vessel and acetone was evaporated at reduced pressure and room temperature to form a 20% solution and then added again to obtain a 10% solution, so as to improve UV stability, according to reference (40). The MS adhesion promoter was applied on the bronze surface by brushing in order to achieve a specific coating weight of  $1.5 \text{ g m}^{-2}$  (30 mg of solution on each sample). In the case of the MS coating (B-MS and P-MS), only the sol-gel primer was applied without applying the fluoroacrylate top coating, as the epoxy stiffener block used in the three-point bending test was not sufficiently adherent to the top layer for the proper execution of the adherence measurements.

4. Incralac was purchased from Bresciani s.r.l. ([www.brescianisrl.it](http://www.brescianisrl.it)) and was sprayed onto both the B and the P samples as a 3 wt% solution in an ethyl acetate solvent, in order to achieve a specific coating weight of about  $6 \text{ g m}^{-2}$ .

All these coatings were applied to both the bare (B) and the patinated (P) bronze coupons, except for PropS-SH with the MPT-CD complex (PropS-SH-

**Table 1: Overview of the selected coatings for the protection of outdoor bronzes**

Coating type	Acronym	Designation	Components	Application mode	Thickness ( $\mu\text{m}$ )
Incralac® commercial coating	Inc	Incralac® (reference)	3 wt% in ethyl acetate	Spraying	3-6
Alkyl-silane	PropS-SH	Silane without inhibitor	PropS-SH (3-mercaptopropyltrimethoxysilane)	Spraying	3-6
	PropS-SH-MPT	Silane with corrosion inhibitor	PropS-SH with MPT (5-mercaptopentyl-tetrazole)/CD ( $\beta$ -cyclodextrin) complex	Spraying	3-6
Sol-gel (oxysilane)	SG	Sol-gel coating (HMFS-GPTMS-MTMS-2)	HMFS-GPTMS-MTMS-2 3-glycidoxypropyltrimethoxysilane (GPTMS) with hexamethyldisilazane-treated silica particles (HMFS) and methyltrimethoxysilane (MTMS)	Spraying	<1
	MS	Sol-gel primer MS only applied here (without final fluoropolymer application)	Copolymer of methyl methacrylate and methacryloxypropyltrimethoxysilane (MS)	Brushing	<2

MPT), which was applied only to the bare bronze. In fact, the entrapment of this complex in PropS-SH<sup>41,42</sup> did not improve the coating durability in the case of the P bronze samples during exposures to artificial acid rain as had been initially expected, whereas it was effective in the case of naturally aged bare bronze.<sup>43</sup>

The substrate coupons ( $10 \times 50 \times 0.5 \text{ mm}^3$ ) were obtained by die cutting the rolled bronze plates. In the case of the bare metallic samples (B), the coatings were applied to the coupons which had been polished up to 1200P (SiC) and then ethanol-rinsed. In the case of the patinated coupons (P), the protective coatings were applied directly to the black patina. Preliminary optical investigation confirmed the macroscale homogeneity of all the coatings before aging.

### The aging method

In order to assess the level of protection against corrosion provided by the different coatings, the coated bronze coupons were aged by immersion for 28 days in a synthetic acid rain (AR) solution, which was concentrated by a factor of 10 with respect to the composition of natural acid rain collected during winter months in Bologna and used as a reference.<sup>34,35,44</sup> The concentrated AR solution (which had a pH of 3.3 and a conductivity of  $345 \mu\text{S}/\text{cm}$  at  $25^\circ\text{C}$ ) had the following composition:  $14.4 \text{ mg L}^{-1} \text{ CaSO}_4 \cdot 2\text{H}_2\text{O}$ ;  $15.0 \text{ mg L}^{-1} (\text{NH}_4)_2\text{SO}_4$ ;  $19.1 \text{ mg L}^{-1} \text{ NH}_4\text{Cl}$ ;  $15.1 \text{ mg L}^{-1} \text{ NaNO}_3$ ;  $39.3 \mu\text{L L}^{-1} \text{ HNO}_3$  (65 wt%);  $3.2 \text{ mg L}^{-1} \text{ CH}_3\text{COONa}$ ;  $0.8 \text{ mg L}^{-1} \text{ HCOONa}$ . The concentrated AR solution can slightly accelerate the corrosion of bronze with respect to plain synthetic rain due to its lower pH value (3.3 instead of 4.3) and higher electrical conductivity. Before immersion in the aging solution, the edges of each coupon were coated with a protective varnish in order to prevent loss of adhesion due to corrosion underneath the coating. All tests were carried out on at least 4 coupons.

### Practical adhesion measurements

The adherence measurement method by means of the three-point bending, which is described in references (6) and (24), was carried out according to the standard ISO 14679-1997. The experimental procedure includes the mounting of a stiffener quadrangular block directly onto each coated coupon ( $10 \text{ mm} \times 50 \text{ mm}$ ). It should be noted that a die cutting apparatus was used to avoid mechanical deformation and burring along any of the edges. By means of a silicon mold that has been specifically adapted for obtaining  $25 \times 5 \times 4 \text{ mm}^3$  stiffener epoxy block(s), the injection of 0.5 mL liquid adhesive (Araldite AY103-HY991) was performed as depicted in Fig. 2. After polymerization at ambient temperature ( $23^\circ\text{C}$ ) for 24 h, the mounted sample was placed in a dry oven at  $60^\circ\text{C}$  for 2 h.

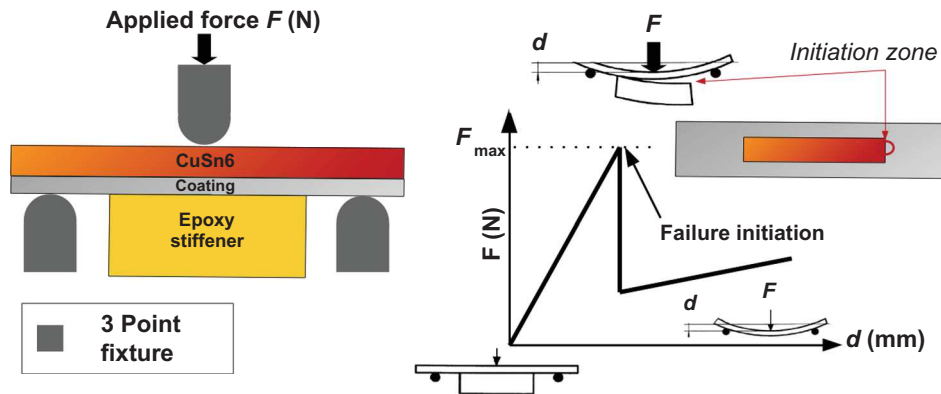


Fig. 2: Three-point bending test for practical adhesion (adherence) measurements: (left) position of the sample in the testing configuration and (right) typical load–deformation curve: the marked change in slope corresponds to the initiation of failure in the coated surface at the border of the stiffener block

Table 2: Practical adhesion (or adherence) data ( $F_{max}$ ) for the bare (B) samples, before and after artificial aging (28-day immersion in tenfold concentrated acid rain)

Designation	Acronym	Before aging			After aging		
		$F_{max}$ (N)	SD	Failure type	$F_{max}$ (N)	SD	Failure type
Bare Incolac <sup>®</sup>	B-Inc	23.3	± 2.2	Cohesive	13	± 2.8	Adhesive
Bare PropS-SH	B-PropS-SH	36.9	± 4.2	Adhesive	26	± 3.0	Adhesive
Bare PropS-SH-MPT	B-PropS-SH-MPT	32	± 3.1	Adhesive	20	± 2.2	Adhesive
Bare sol-gel	B-SG	18.2	± 0.3	Adhesive	20	± 3.1	Adhesive
Bare MS	B-MS	10.1	± 1.5	Adhesive	5	± 5	Adhesive

An Instron<sup>®</sup> 3367 tensile testing machine fitted with a 500-N full-scale load cell, with a sensitivity of  $\pm 0.5\%$  of the measured values and a crosshead displacement speed of  $0.5 \text{ mm min}^{-1}$ , was used in the three-point bending test configuration (Fig. 2, left). The apparatus parameters were controlled by the Bluehill software (Instron<sup>®</sup>). The stiffened sample was positioned in order to record the mechanical behavior of the coating under an increasing load, up to its adhesive failure (the coating/(B or P) bronze interface), marked by a clearly visible rupture on the load–deformation  $F(N)$ - $d(\text{mm})$  curve (Fig. 2, right). The performance of the measurements followed the provisions of the standard ISO 14679-1997, but with a modification in the spacing between the two lower support points, which was changed from the 33 mm given in the standard to 35 mm in the real experimental conditions corresponding to the ergonomic adaptation of the used device.

The ultimate load  $F_{max}$  was directly proportional to the adherence of the coating on the metal substrate. The measurements are validated by testing a set of 6 coupons before aging and 4 after aging for each system. Each value (given in Tables 2 and 3) corresponds to

the average and the standard deviation for each set of samples.

#### Adhesive failure observation and surface characterization

After the three-point bending test had been performed, all the samples were optically observed in order to precisely locate the region and type of failure: adhesive (at the interface between patina layers or at the interface with the bronze substrate) or cohesive [within one of the surface layers (either the coating or the patina)].

The optical examination work was carried out by means of a ZEISS STEMI binocular and an AxioVision V16 stereomicroscope. Specific observations of the coating failure on the bare and black-patinated samples (before and after aging) were also performed by scanning electron microscope (SEM FEI Helios NanoLab 600i) coupled with energy-dispersive spectroscope (EDS—Aztec Oxford apparatus, SSD detector, WD 4 mm). After SEM examination of the coated

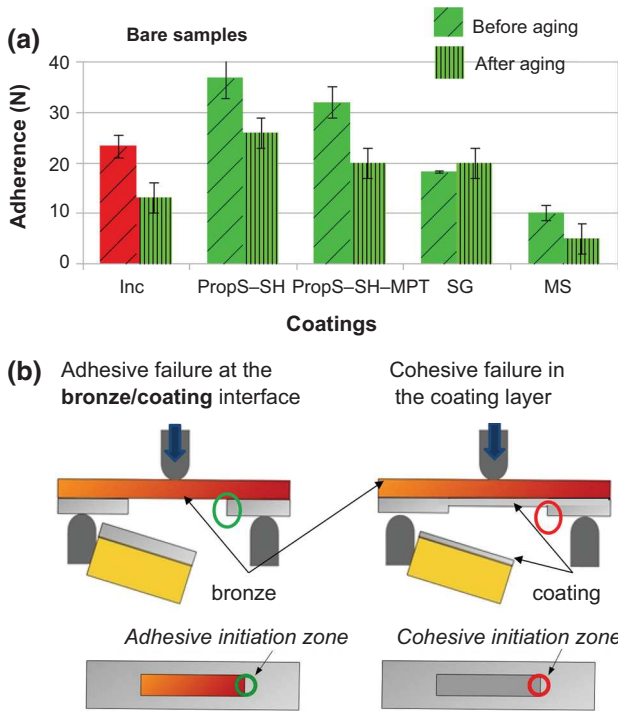


**Fig. 3: Coated bare Cu-6Sn bronze.** (a) Adherence (practical adhesion) test results obtained before and after aging. The color of histogram columns indicates the failure mode: adhesive failure at the bronze/coating interface (green) or cohesive failure within the coating (red), as schematized in (b) where both side view (top) and surface view (bottom) of the tested sample are shown for each failure mode (adhesive vs. cohesive) (Color figure online)

surfaces, in situ cross sections were created in some significant areas, applying focused ion beam (FIB) milling with Ga<sup>+</sup> ions as described in reference (34).

## Results and discussion

During the tests, it was found that the displacement  $d$  increases proportionally to the applied load  $F$ , as is shown in Fig. 2b.<sup>6,23-25</sup> Since the failure load took place in the elastic domain, the maximum load corresponding to the breaking load  $F_{max}$  (i.e., the load at failure) can be considered to be well representative of practical adhesion. Low  $F_{max}$  standard deviation values (< 10%) were achieved, with the exception of data for the coated patinated bronze test specimens after accelerated aging, which is discussed in the “After accelerated aging” section.

### Coated bare bronze (B)

The practical adhesion data ( $F_{max}$ ) for the protective coatings on bare bronze (B), before and after accelerated aging, are summarized in Table 2 and presented in Fig. 3a. Two types of failure, which are schematically presented in Fig. 3b, were identified: adhesive failure at the metal/coating interface (shown by green columns in the histogram of Fig. 3a) and cohesive failure within the coating (shown by red columns).

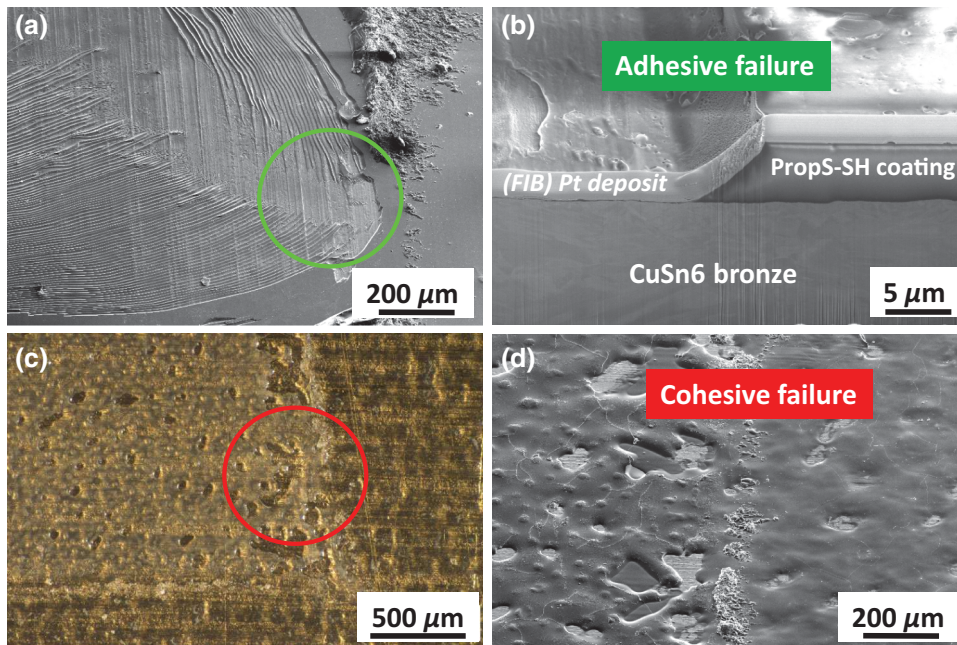


**Fig. 4: Coated bare bronze before aging: morphological observations after performance of the three-point bending test.** Adhesive failure: (a) PropS-SH coating, initiation zone, and (b) FIB-SEM cross section. Cohesive failure: Incralac<sup>®</sup>, (c) optical and (d) SE images of the initiation zone

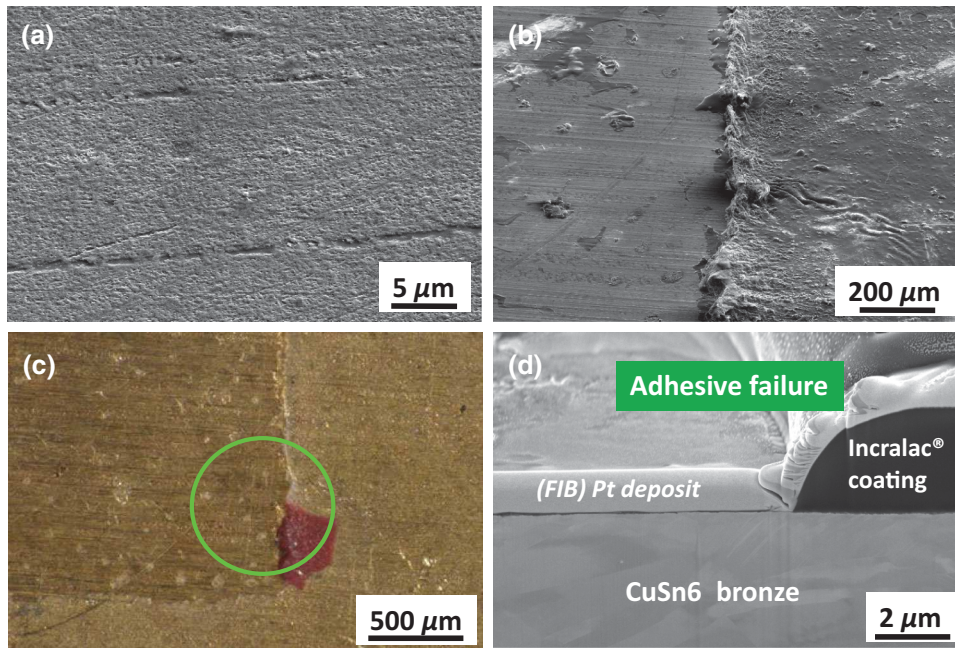


**Fig. 5: Coated bare bronze after aging (28-day immersion in concentrated acid rain): morphological observation after performance of the three-point bending test. (a) PropS-SH coating. (b) Incralac<sup>®</sup>: adhesive failure (SE) and (c) optical images of the surface, (d) FIB-SEM cross section in the failure zone; in (c), the red point indicating the initiation zone was made by a pencil (Color figure online)**

#### *Before accelerated aging*

In the case of the bare samples before aging (Fig. 3a), the failure load  $F_{\max}$  clearly changes with the applied coating.  $F_{\max}$  is the highest for the PropS-SH coatings (36.9 N) and lowest for the MS coating (10.1 N), which was applied as a sol-gel primer for the fluoropolymer top layer. Apart from Incralac, all the coated systems underwent adhesive failure at the bronze/coating interface. This morphology is illustrated in Fig. 4 for the PropS-SH coating, for which the adhesive failure zone (marked by a green circle in Fig. 4a) revealed marked disruption of the polymer. Failure of the polymer at the bronze/polymer interface is clearly shown by the FIB cross sections (Fig. 4b). The addition of the inhibitor complex ( $\beta$ -cyclodextrin, Table 1) in PropS-SH-MPT did not modify the failure morphology in comparison with the plain PropS-SH and only negligibly impaired the coating adherence (Table 2).

On the other hand, the Incralac<sup>®</sup> coating when applied to the bare samples exhibited a cohesive failure within the coating layer, at a relatively low  $F_{\max}$  (23.3 N). As can be seen in Figs. 4c and 4d, this coating exhibited a number of cracks and delaminated areas.

Before aging, the PropS-SH organosilane coating displayed the best behavior among all the investigated coatings, with high adhesion and cohesion. On the other hand, the reference Incralac<sup>®</sup> coating was highly adherent, but its cohesion was low. The other selected coatings revealed lower resistance to damage during the three-point bending test.

#### *After accelerated aging*

In the case of the aged coatings on bare bronze (B-samples), immersion in concentrated acid rain altered the resistance to damage due to the performance of the three-point bending test: only adhesive failure was observed. As shown in Fig. 3a, the aging led to a marked decrease in the maximum load values  $F_{\max}$  for all the coatings, except for the SG coating (sol-gel oxysilane, Table 1) which maintained a practical adhesion of about 20 N.

The surface of the coatings was modified by the exposure to concentrated acid rain and revealed microcracks and increased roughness, as can be seen in Figs. 5a and 5b for the PropSH and Incralac<sup>®</sup> coatings, respectively. In the case of the aged samples, no color variation of the bronze substrate was optically detected under the coating after failure, as can be seen, for example, in Fig. 5c for Incralac<sup>®</sup>. This means that the measured decrease in adhesive adherence was not connected to any significant reduction in any mechanical property within the coating, nor to any coating detachment induced by the growth of corrosion products. Thus, failure cannot be due to corrosion of the bronze substrate, as was confirmed by SEM observation and the FIB-SEM cross sections (Fig. 5d). Due to aging, water, oxygen, and possibly chlorides diffusion occurred quite slowly at negligible corrosion rates, but could have reduced the coating/bronze substrate bonding. Thus, in the case of all the aged coatings the decrease in adherence can be ascribed to the damage of the bare bronze/coating interface, either with the

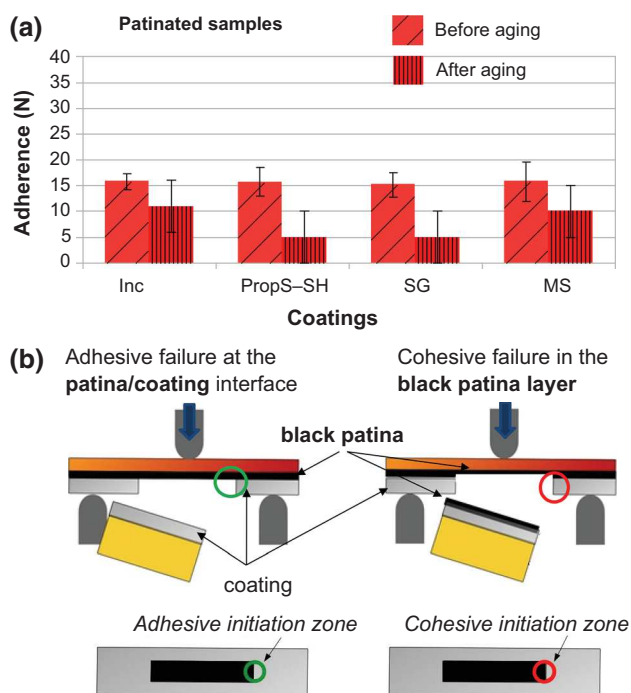


**Fig. 6: Coated patinated Cu-6Sn bronze. (a) Adherence (practical adhesion) test results obtained before and after aging: the color of histogram columns indicates the failure mode: adhesive failure at the black patina/coating interface (green) or cohesive failure within the black patina (red), as schematized in (b) where both side view (top) and surface view (bottom) of the tested sample are shown for each failure mode (adhesive vs. cohesive). The histogram with red columns in (a) shows that only cohesive failure within the black patina layer occurred (Color figure online)**

break of covalent bond at the interface (chemical theory of adhesion) or with the plasticization of the first polymer layer (weak boundary layer adhesion theory<sup>14,15</sup>).

### Coated patinated bronze (P)

The practical adhesion data ( $F_{max}$ ) for the coated patinated samples (coated P samples), before and after aging, are summarized in Table 3, and the results are reported in Fig. 6a. When compared to the coated bare bronze test specimens, markedly different behavior can be observed: only cohesive failures (marked by red columns in the histogram of Fig. 6b) occurred, with no adhesive failure (green columns).

#### Before accelerated aging

In the case of the coated patinated samples before aging, comparable  $F_{max}$  values of about 15 N were obtained for all the coatings, with good repeatability (Table 3). A very similar  $F_{max}$  value of  $13.8 \pm 1.3$  N

was also obtained for the uncoated, black-patinated coupons. This means that the results of the three-point bending measurement were mostly affected by the presence of the black patina layer on the bronze substrate: cohesion of the artificial patina is thus likely to be the main weakness of the coated system.

This assumption was demonstrated by the SEM observations which were performed on the coated patinated substrates. As shown in Fig. 7 for Incralac<sup>®</sup> (Figs. 7a and 7b), PropS-SH (Figs. 7c and 7d) and the fluoropolymer primer MS (Figs. 7e and 7f), the failure was always cohesive, revealing the internal layer of the black patina, characterized by the presence of cuprous oxide (whereas the external layer mostly consists of cuprous sulfide, Figs. 1c and 1d). Based on detailed observations at higher magnification (Figs. 7d and 7e) and on the FIB-SEM cross sections (Figs. 7b and 7f), the porous patina revealed some internal microcracking which can be filled up by the polymeric coating. However, this is not enough if a cohesive failure within the patina is to be avoided during the bending test. Cohesive failure can occur either in the external cuprous sulfide layer of the patina, such as the Incralac<sup>®</sup> coated samples (Fig. 7b), or within the internal cuprous oxide layer, such as the PropS-SH (Fig. 7d) as well as the MS (Figs. 7e and 7f). Thus, in the case of the patinated bronze test specimens, the behavior of the patina, which is a weak layer, plays a dominant role, so it was not possible to assess the practical adhesion of the coatings to the patina.

#### After accelerated aging

The results after aging for the patinated bronze test specimens are given Table 3 and are reported in Fig. 6a. Similarly to the results for the coated bare bronze after aging, there was a considerable decrease in  $F_{max}$  after immersion in the concentrated acid rain solution, but here all the aged coatings appeared to have only weak adherence. A low repeatability of measurements was observed. Failure was always cohesive within the patina for all the coatings revealing the internal patina layer, as is shown in Fig. 8. This behavior can be attributed to the behavior of the coatings during aging, inducing microcracking as shown for Incralac<sup>®</sup> and PropS-SH (Figs. 8b and 8d, respectively), but also to an increase in the surface roughness, as observed for PropS-SH and MS (Figs. 8d and 8e, respectively). This modification of the coating could involve an increase in coating flaws and porosity and could affect the black patina integrity, allowing the transformation of copper sulfide to cuprous oxide, as described in the case of the black-patinated Cu-Si-Mn bronze exposed to acid rain.<sup>34</sup> As shown in Fig. 8, when the three-point bending test was applied to the accelerated aging samples, they systematically induce cohesive failure within the internal part of the black patina. This is typically illustrated by the optical observation shown in Fig. 8a, in which the brown/dark

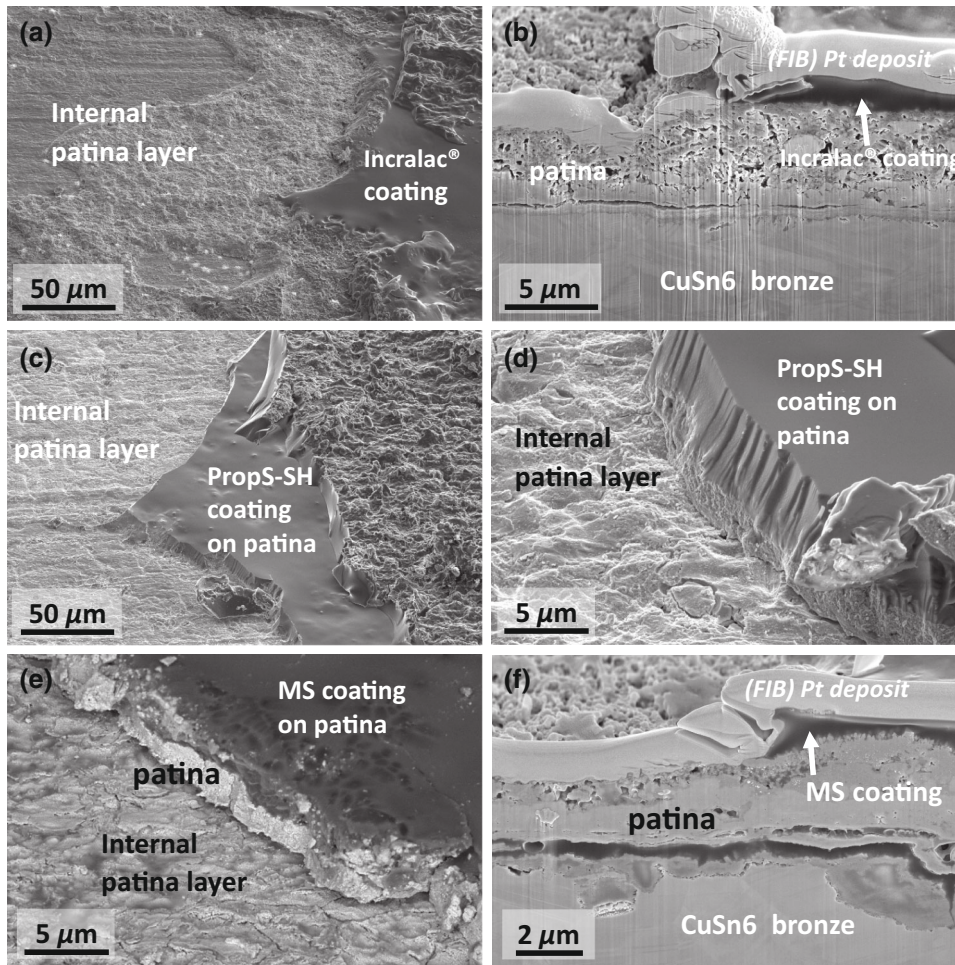


**Fig. 7: Coated patinated bronze before aging: (a) SEM at the surface of the coating failure. Incralac, (b) FIB-SEM cross section of the Incralac system; (c) and (d) PropS-SH; (e) surface failure of MS coating, and (f) FIB-SEM cross section of the MS coating system**

yellow internal layer of the patina is clearly visible on the left-hand side of the image. From the FIB cross section shown in Fig. 8f, in the failure zone only the internal layer of the black patina still remains on the bronze substrate, while the external layer of the patina has peeled off together with the overlying polymeric coating, which is therefore not visible in Fig. 8f. In this figure, an internal crack at the internal patina/bronze interface can also be observed. It could be the result of the action of initial stresses induced by the heating during the patina-making or by the bending test itself, but it can be seen that the adhesion of this inner part of the black patina to the underlying bronze remains higher than the cohesion of the multilayered structure of the black patina as previously described.

Thus accelerated aging clearly has an effect on the practical adhesion of coatings applied to black-patinated bronze. In fact, aging negatively affects the properties of both the polymeric coating and thus of the underlying artificial patina, favoring cohesive failure within the internal part of the patina. The  $F_{max}$

values are directly related to the aged patina itself, almost regardless of the coating applied.

These results support the conclusion that the artificial black patina plays a major role in the protective behavior of coatings on patinated bronze in outdoor conditions. Practical adhesion of the coatings is affected by the behavior of the patina during aging and in turn is affected by the ability of the polymeric coatings to act as a barrier toward an aggressive environment. These results also confirm the conclusion that a full “coating-patina-bronze” system must be taken into account when carrying out practical adhesion measurements.

## Conclusions

This work allowed for a methodological approach for measuring adherence property of coatings on (patinated) bronze based on a high-accuracy test.

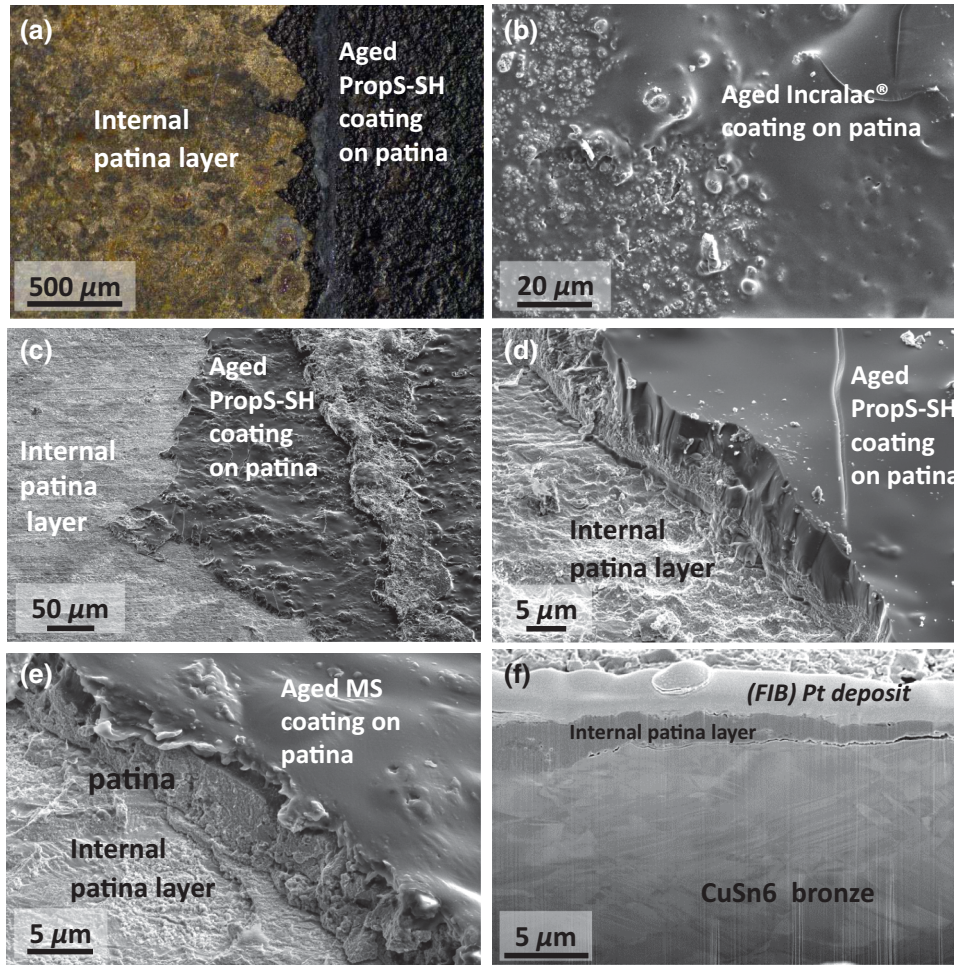


**Fig. 8:** Coated patinated bronze after aging (28-day immersion in tenfold concentrated acid rain). PropS-SH: (a) optical observation of cohesive failure, revealing the internal patina layer (light brown, on the left-hand side); (b) SEM observation of Incralac<sup>®</sup>, revealing some cracks on the surface of the coated, black-patinated bronze; (c) and (d) surface images of PropS-SH, showing cohesive failure after aging; (e) surface image of MS, showing cohesive failure, and (f) FIB-SEM cross section of the MS coating system

**Table 3: Practical adhesion (or adherence) data ( $F_{max}$ ) for the patinated (P) samples, before and after artificial aging (28-day immersion in tenfold concentrated acid rain)**

Designation	Acronym	Before aging			After aging		
		$F_{max}$ (N)	SD	Failure type	$F_{max}$ (N)	SD	Failure type
Patinated Incralac <sup>®</sup>	P-Inc	15.8	± 1.5	Cohesive	11	± 5	Cohesive
Patinated PropS-SH	P-PropS-SH	15.7	± 2.8	Cohesive	5	± 5	Cohesive
Patinated sol-gel	P-SG	15.2	± 2.4	Cohesive	5	± 5	Cohesive
Patinated MS	P-MS	15.8	± 3.9	Cohesive	10	± 5	Cohesive

Thus, the practical adhesion of selected protective coatings applied to tin bronze (Cu-6Sn) for outdoor monuments has been determined by means of the three-point bending test, taking into account a commercially available protective coating (Incralac<sup>®</sup>), which has been widely used for bronze conservation,

as a reference for comparison. The investigations were performed on coatings that were applied to the bare alloy as well as to black K<sub>2</sub>S-patinated surfaces, prepared in the traditional nineteenth-century manner. The testing method applied here was used for the first time to assess the effectiveness of protective coatings

applied to bronze within the context of cultural heritage conservation. The three-point bending test is based on a standardized method which permits the performance of quantitative, repeatable and consistent measurements of adhesion strength ( $F_{\max}$ ), avoiding approaches only based on qualitative evaluations.

The measurements were performed before and after accelerated aging (28-day immersion in tenfold concentrated acid rain).

In the case of the bare Cu–6Sn substrates, all the coatings underwent adhesive failure at the bronze/coating interface, except for Incralac<sup>®</sup> which showed cohesive failure within the coating itself. Accelerated aging resulted in a significant decrease in the measured practical adhesion. The best behavior was observed in the case of the silane coatings (PropSH and PropS-SH-MPT), which were more adherent than the Incralac<sup>®</sup> reference coating.

In the case of the black-patinated Cu–6Sn bronze test specimens, cohesive failure always occurred within the patina. All the coatings had similar  $F_{\max}$  values with high standard deviation. All the tested coatings showed practical adhesion to the patina which was higher than the cohesion of the patina itself. This underlines the question of the quality and property of the patina applied on bronze. After the aging test in concentrated acid rain had been performed, there was a clear decrease in the cohesion of the patina, due to a partial loss in the protective effectiveness of the coatings.

From a methodological point of view, these results underline the importance of carrying out accurate practical adhesion measurements, taking into account the full “coating-patina-alloy” system, in order to obtain a proper evaluation of the protective behavior of selected coatings for the conservation of ancient and historic metals.

**Acknowledgments** This work was performed within the scope of the M-Era.Net European project BIMPACT, which was supported by national funding organizations (MIZS-Slovenia, MIUR-Italy, RMP-France). Special thanks are due to Nina Gartner for her constant administrative help during the implementation of this project.

## References

1. Texier, A, Azema, A, “Open Air Metal—Outdoor Metallic Sculpture from the 19th to the Early 20th Century: Identification, Conservation, Restoration.” *Int. Conf. 2014 SF-IIC/ICOMOS*, p 288, Paris (2015)
2. Pilz, M, Römich, H, “Sol–Gel Derived Coating for Outdoor Bronze Conservation.” *J. Sol-Gel Sci. Technol.*, **8** 1071–1075 (1997). <https://doi.org/10.1007/BF02436986>
3. Brunoro, G, Frignani, A, Colledan, A, Chiavari, C, “Organic Films for Protection of Copper and Bronze Against Acid Rain Corrosion.” *Corros. Sci.*, **45** 2219–2231 (2003). [https://doi.org/10.1016/S0010-938X\(03\)00065-9](https://doi.org/10.1016/S0010-938X(03)00065-9)
4. Kosec, T, Legat, A, Milošev, I, “The Comparison of Organic Protective Layers on Bronze and Copper.” *Prog. Org. Coat.*, **69** 199–206 (2010). <https://doi.org/10.1016/J.PORGCOAT.2010.04.010>
5. Chiavari, C, Balbo, A, Bernardi, E, Martini, C, Bignozzi, MC, Abbottoni, M, Monticelli, C, “Protective Silane Treatment for Patinated Bronze Exposed to Simulated Natural Environments.” *Mater. Chem. Phys.*, **141** 502–511 (2013). <https://doi.org/10.1016/J.MATCHEMPHYS.2013.05.050>
6. Floch, V, Doleyres, Y, Amand, S, Aufray, M, Pébère, N, Verchère, D, “Adherence Measurements and Corrosion Resistance in Primer/Hot-Dip Galvanized Steel Systems.” *J. Adhes.*, **89** 339–357 (2013). <https://doi.org/10.1080/00218464.2013.757510>
7. Olivier, MG, Romano, AP, Vandermiers, C, Mathieu, X, Poelman, M, “Influence of the Stress Generated During an Ageing Cycle on the Barrier Properties of Cathodic Coatings.” *Prog. Org. Coat.*, **63** 323–329 (2008). <https://doi.org/10.1016/j.porgcoat.2008.01.018>
8. Le Manchet, S, Landoulsi, J, Richard, C, Verchère, D, “Study of a Chromium-Free Treatment on Hot-Dip Galvanized Steel: Electrochemical Behaviour and Performance in a Saline Medium.” *Surf. Coat. Technol.*, **205** 475–482 (2010). <https://doi.org/10.1016/j.surfcoat.2010.07.009>
9. Miszczyk, A, Darowicki, K, “Multispectral Impedance Quality Testing of Coil-Coating System Using Principal Component Analysis.” *Prog. Org. Coat.*, **69** 330–334 (2010). <https://doi.org/10.1016/j.porgcoat.2010.07.003>
10. Bajat, JB, Popić, JP, Mišković-Stanković, VB, “The Influence of Aluminium Surface Pretreatment on the Corrosion Stability and Adhesion of Powder Polyester Coating.” *Prog. Org. Coat.*, **69** 316–321 (2010). <https://doi.org/10.1016/j.porgcoat.2010.07.004>
11. Ramezanzadeh, B, Attar, MM, “An Evaluation of the Corrosion Resistance and Adhesion Properties of an Epoxy-Nanocomposite on a Hot-Dip Galvanized Steel (HDG) Treated by Different Kinds of Conversion Coatings.” *Surf. Coat. Technol.*, **205** 4649–4657 (2011). <https://doi.org/10.1016/j.surfcoat.2011.04.001>
12. Akid, R, Gobara, M, Wang, H, “Corrosion Protection Performance of Novel Hybrid Polyaniline/Sol-Gel Coatings on an Aluminium 2024 Alloy in Neutral, Alkaline and Acidic Solutions.” *Electrochim. Acta*, **56** 2483–2492 (2011). <https://doi.org/10.1016/j.electacta.2010.12.032>
13. Bull, SJ, Berasetegui, EG, “Chapter 7: An Overview of the Potential of Quantitative Coating Adhesion Measurement by Scratch Testing.” *Tribol. Int.*, **39** 99–114 (2006). <https://doi.org/10.1016/j.triboint.2005.04.013>
14. Mittal, KL, “Adhesion Measurement of Thin Films.” *Electrocompon. Sci. Technol.*, **3** 21–42 (1976). <https://doi.org/10.1155/APEC.3.21>
15. Brown, SD, “Adherence Failure and Measurement: Some Troubling Questions.” In: Mittal, KL (ed.) *Adhesion Measurement of Films and Coatings*, pp. 15–39. VSP, Utrecht (1995)
16. I. 20502 Standard, Fine Ceramics (Advanced Ceramics, Advanced Technical Ceramics)—Determination of Adhesion of Ceramic Coatings by Scratch Testing, 2005
17. Noh, SM, Lee, JW, Nam, JH, Park, JM, Jung, HW, “Analysis of Scratch Characteristics of Automotive Clearcoats Containing Silane Modified Blocked Isocyanates via Carwash and Nano-scratch Tests.” *Prog. Org. Coat.*, **74** 192–203 (2012). <https://doi.org/10.1016/j.porgcoat.2011.12.009>

18. Malzbender, J, den Toonder, JMJ, Balkenende, AR, de With, G, "Measuring Mechanical Properties of Coatings: A Methodology Applied to Nano-particle-Filled Sol-Gel Coatings on Glass." *Mater. Sci. Eng. R Rep.*, (2002). [https://doi.org/10.1016/s0927-796x\(01\)00040-7](https://doi.org/10.1016/s0927-796x(01)00040-7)
19. I. 1518-1 Standard, Paints and Varnishes—Determination of Scratch Resistance—Part 1: Constant-Loading Method (2011)
20. I. 1518-2 Standard, 2011 Paints and Varnishes—Determination of Scratch Resistance—Part 2: Variable-Loading Method (2011)
21. Vaughn, GD, Frushour, BG, Dale, WC, "Scratch Indentation, A Simple Adhesion Test Method for Thin Films on Polymeric Supports." *J. Adhes. Sci. Technol.*, **8** 635–650 (1994). <https://doi.org/10.1163/156856194X00393>
22. Matthews, KHA, *Coatings Tribology, Volume 56: Properties, Mechanisms, Techniques and Applications in Surface Engineering*, 2nd ed. Elsevier Science, Amsterdam (2009)
23. Roche, AA, Dole, P, Bouzziri, M, "Measurement of the Practical Adhesion of Paint Coatings to Metallic Sheets by the Pull-Off and Three-Point Flexure Tests." *J. Adhes. Sci. Technol.*, **8** 587–609 (1994). <https://doi.org/10.1163/156856194X00366>
24. Genty, S, Sauvage, J-B, Tingaut, P, Aufray, M, "Experimental and Statistical Study of Three Adherence Tests for an Epoxy-Amine/Aluminum Alloy System: Pull-Off, Single Lap Joint and Three-Point Bending tests." *Int. J. Adhes. Adhes.*, **79** 50–58 (2017). <https://doi.org/10.1016/j.ijadhadh.2017.09.004>
25. Roche, AA, Behme, AK, Solomon, JS, "A Three-Point Flexure Test Configuration for Improved Sensitivity to Metal/Adhesive Interfacial Phenomena." *Int. J. Adhes.*, **2** 249–254 (1982). [https://doi.org/10.1016/0143-7496\(82\)90032-X](https://doi.org/10.1016/0143-7496(82)90032-X)
26. Zucchi, F, Grassi, V, Frignani, A, Trabanelli, G, "Inhibition of Copper Corrosion by Silane Coatings." *Corros. Sci.*, **46** 2856–2865 (2004). <https://doi.org/10.1016/j.corsci.2004.03.019>
27. Monticelli, C, Grassi, V, Martini, C, Chiavari, C, Mavilia, G, Zanotto, F, Masi, G, Bernardi, E, "Protectiveness of Different Silane Coatings on Patinated Ancient and Modern Bronzes: Part 1." In: *EUROCORR 2017 20th ICC Process Saf. Congr. 2017, Eur. Fed. Corros.* Event No. 417, Prague (Czech Republic), 2017: p. Paper n. 82171
28. Masi, G, Martini, C, Bernardi, E, Bignozzi, MC, Monticelli, C, Balbo, A, Zanotto, F, Aufray, M, Josse, C, Esvan, J, Robbiola, L, "Protectiveness of Different Silane Coatings on Patinated Ancient and Modern Bronzes: Part 2." In: *EUROCORR 2017 20th ICC Process Saf. Congr. 2017, Eur. Fed. Corros.* Event No. 417, Prague (Czech Republic), 2017 Paper n. 95722
29. Bescher, E, Mackenzie, JD, "Sol-Gel Coatings for the Protection of Brass and Bronze." *J. Sol-Gel Sci. Technol.*, **26** 1223–1226 (2003)
30. Ebnesajjad, S, "Applied Plastics Engineering Handbook." In: Kutz, M (ed.) *Applied Plastics Engineering Handbook*. Elsevier Inc., Amsterdam (2011) <https://doi.org/10.1016/c2010-0-67336-6>
31. Picard, L, Phalip, P, Fleury, E, Ganachaud, F, "Chemical Adhesion of Silicone Elastomers on Primed Metal Surfaces: A Comprehensive Survey of Open and Patent Literatures." *Prog. Org. Coat.*, **80** 120–141 (2015). <https://doi.org/10.1016/j.porgcoat.2014.11.022>
32. Marabelli, M, Napolitano, G, "Nuovi sistemi protettivi applicabili su opere o manufatti in bronzo esposti all'aperto TT—New Protective Systems Applied to Outdoor Bronze Statuary or Artifacts." *Materiali e Strutture*, **1–2** 51–58 (1991)
33. Weil, PD, "A review of the history and practice of patination." In: Floyd Brown, B, N.B. of S. United States. (Eds.), *Corros. Met. Artifacts a Dialog between Conservators. Archaeologists and Corrosion*, pp. 77–92. Scientists, NBS Special Publication 479, Washington D.C. (1977)
34. Masi, G, Josse, C, Esvan, J, Chiavari, C, Bernardi, E, Martini, C, Bignozzi, MC, Monticelli, C, Zanotto, F, Balbo, A, Svara Fabjan, E, Kosec, T, Robbiola, L, "Evaluation of the Protectiveness of an Organosilane Coating on Patinated Cu-Si-Mn Bronze for Contemporary Art." *Prog. Org. Coat.*, **127** 286–299 (2019). <https://doi.org/10.1016/j.porgcoat.2018.11.027>
35. Chiavari, C, Bernardi, E, Martini, C, Passarini, F, Ospitali, F, Robbiola, L, "The Atmospheric Corrosion of Quaternary Bronzes: The Action of Stagnant Rain Water." *Corros. Sci.*, **52** 3002–3010 (2010). <https://doi.org/10.1016/j.corsci.2010.05.013>
36. Chiavari, C, Bernardi, E, Balbo, A, Monticelli, C, Raffo, S, Bignozzi, MC, Martini, C, "Atmospheric Corrosion of Fire-Gilded Bronze: Corrosion and Corrosion Protection During Accelerated Ageing Tests." *Corros. Sci.*, **100** 435–447 (2015). <https://doi.org/10.1016/J.CORSCI.2015.08.013>
37. Sidot, E, Kahn-Harari, A, Cesari, E, Robbiola, L, "The Lattice Parameter of  $\alpha$ -Bronzes as a Function of Solute Content: Application to Archaeological Materials." *Mater. Sci. Eng. A*, **393** 147–156 (2005). <https://doi.org/10.1016/J.MSEA.2004.10.001>
38. Ropret, P, Kosec, T, "Raman Investigation of Artificial Patinas on Recent Bronze—Part I: Climatic Chamber Exposure." *J. Raman Spectrosc.*, **43** 1578–1586 (2012). <https://doi.org/10.1002/jrs.4068>
39. Masi, G, Esvan, J, Josse, C, Chiavari, C, Bernardi, E, Martini, C, Bignozzi, MC, Gartner, N, Kosec, T, Robbiola, L, "Characterisation of Typical Patinas Simulating Bronze Corrosion in Outdoor Conditions." *Mater. Chem. Phys.*, **200** 308–321 (2017). <https://doi.org/10.1016/j.matchemphys.2017.07.091>
40. Deanin, RD, Orroth, SA, Eliassen, RW, Greer, TN, "Mechanism of Ultraviolet Degradation and Stabilization in Plastics." *Polym. Eng. Sci.*, **10** 228–234 (1970). <https://doi.org/10.1002/pen.760100408>
41. Khramov, AN, Voevodin, NN, Balbyshev, VN, Donley, MS, "Hybrid Organo-Ceramic Corrosion Protection Coatings with Encapsulated Organic Corrosion Inhibitors." *Thin Solid Films*, **447–448** 549–557 (2004). <https://doi.org/10.1016/j.tsf.2003.07.016>
42. Khramov, AN, Voevodin, NN, Balbyshev, VN, Mantz, RA, "Sol-Gel-Derived Corrosion-Protective Coatings with Controllable Release of Incorporated Organic Corrosion Inhibitors." *Thin Solid Films*, **483** 191–196 (2005). <https://doi.org/10.1016/j.tsf.2004.12.021>
43. Monticelli, C, Grassi, V, Mavilia, G, Zanotto, F, "Entrapment of Corrosion Inhibitors in Silane Coatings to Improve Bronze Corrosion Protection." In: *EUROCORR 2017 20th ICC Process Saf. Congr. 2017, Eur. Fed. Corros.* Event No. 417, Prague (Czech Republic), 2017 Paper n. 82386
44. Bernardi, E, Chiavari, C, Lenza, B, Martini, C, Morselli, L, Ospitali, F, Robbiola, L, "The Atmospheric Corrosion of Quaternary Bronzes: The Leaching Action of Acid Rain." *Corros. Sci.*, **51** 159–170 (2009). <https://doi.org/10.1016/J.CO RSCI.2008.10.008>

**Publisher's Note** Springer Nature remains neutral with regard to jurisdictional claims in published maps and institutional affiliations.